

## An Investigation into III-V Infrared Avalanche Photodiodes

J. S. Ng, L. Tan, J. P. R. David, G. J. Rees, C. H. Tan, K. M. Groom and M. Hopkinson  
The University of Sheffield  
Department of Electronic and Electrical Engineering  
Mappin Street, Sheffield, S1 3JD, UK

### Abstract

*Pure electron induced avalanche multiplication and excess noise have been measured at room temperature on a series of InP and  $Al_{0.48}In_{0.52}As$   $p^+ - i - n^+$  diodes. Breakdown voltages deduced from measurements of multiplication as a function of reverse bias are slightly lower in the InP diodes than in  $Al_{0.48}In_{0.52}As$ . However,  $Al_{0.48}In_{0.52}As$  offers lower excess noise than InP in devices with thin avalanche regions. The choice of either material for the avalanche region in a near IR avalanche photodiode will not affect room temperature operating voltage or dependence of gain on bias significantly. However excess avalanche noise can be reduced if InP is replaced with  $Al_{0.48}In_{0.52}As$  in the avalanche region.*

*Keywords: IR Detectors, Impact Ionisation, Avalanche Photodiodes*

### Introduction

Since the internal gain provided by impact ionisation in an avalanche photodiode (APD) can improve the signal to noise ratio of the overall detection system these devices are commonly used in receiver modules in high speed, long range fibre-optic communication systems. Such applications require only discrete APDs sensitive in the near IR, however the capability of integration into a 2D array is essential for imaging applications.

This project aims to design and demonstrate APDs with the capability of integration into a 2D array for applications in (i) rapid, high sensitivity imaging of a scene weakly illuminated with near IR light and (ii) rapid, high sensitivity range finding in the near IR. Such devices should exhibit low excess avalanche, low dark current and high quantum efficiency. This last feature follows from a high multiplication factor and high absorption efficiency.

III-V APDs with  $In_{0.53}Ga_{0.47}As$  absorption regions (of bandgap  $E_g = 0.75eV$  at room

temperature and lattice-matched to InP) are considered the best candidates for applications in the near IR because of the relatively high optical absorption coefficients of  $In_{0.53}Ga_{0.47}As$  at these wavelengths. InP ( $E_g = 1.35eV$ ) is the material most widely used for the avalanche region.  $Al_{0.48}In_{0.52}As$  (room temperature  $E_g = 1.47eV$ ), which is also lattice-matched to  $In_{0.53}Ga_{0.47}As$ , provides an alternative to InP as the avalanche region material and is increasingly being considered as a substitute for InP in optoelectronic devices.

$Al_{0.48}In_{0.52}As$  may pose fewer device fabrication difficulties than InP since it contains no phosphorous, which has been associated with some high temperature processing problems. However no experimental or theoretical comparison of avalanche multiplication behaviour, essential to the design of an APD, has been made between these two materials because of the absence of reliable ionisation coefficients and ionisation threshold energies which determine avalanche multiplication and excess noise.

In this paper we present a comparison of measurements of multiplication and excess noise on InP and  $\text{Al}_{0.48}\text{In}_{0.52}\text{As}$  diodes with a range of i-region widths.

### Wafer Details and Electrical Characterisation

Homojunction InP  $\text{p}^+\text{-i-n}^+$  wafers (InP1, InP2, InP3, InP4 and InP5) and  $\text{Al}_{0.48}\text{In}_{0.52}\text{As}$   $\text{p}^+\text{-i-n}^+$  wafers (AllnAs1, AllnAs2, AllnAs3 and AllnAs4) were grown by MOCVD and MBE, respectively, on  $\text{n}^+$  InP substrates for impact ionisation characterisation. The InP wafers comprised an  $\text{n}^+$  InP cladding layer, an unintentionally doped InP layer of width  $w$ , and finally a  $\text{p}^+$  InP cladding layer. Similar designs were used for the  $\text{Al}_{0.48}\text{In}_{0.52}\text{As}$  wafers with  $\text{n}^+$  and  $\text{p}^+$   $\text{Al}_{0.48}\text{In}_{0.52}\text{As}$  cladding layers and an unintentionally doped  $\text{Al}_{0.48}\text{In}_{0.52}\text{As}$  layer. The wafers studied in this work are summarised in Table 1.

Wafer	Nominal structures	Estimated $w$ ( $\mu\text{m}$ )
InP1	$2.5\mu\text{m}$ $\text{p}^+\text{-i-n}^+$ diode	2.4
InP2	$1.0\mu\text{m}$ $\text{p}^+\text{-i-n}^+$ diode	0.9
InP3	$0.5\mu\text{m}$ $\text{p}^+\text{-i-n}^+$ diode	0.48
InP4	$0.3\mu\text{m}$ $\text{p}^+\text{-i-n}^+$ diode	0.33
InP5	$0.2\mu\text{m}$ $\text{p}^+\text{-i-n}^+$ diode	0.24
AllnAs1	$1.0\mu\text{m}$ $\text{p}^+\text{-i-n}^+$ diode	1.0
AllnAs2	$0.5\mu\text{m}$ $\text{p}^+\text{-i-n}^+$ diode	0.5
AllnAs3	$0.1\mu\text{m}$ $\text{p}^+\text{-i-n}^+$ diode	0.1
AllnAs4	$1.0\mu\text{m}$ $\text{p}^+\text{-i-n}^+$ diode	1.0

Table 1: Summary of InP and  $\text{Al}_{0.48}\text{In}_{0.52}\text{As}$   $\text{p}^+\text{-i-n}^+$  wafers grown for impact ionisation characterisation.

Circular mesa devices of different radii ( $200\mu\text{m}$ ,  $100\mu\text{m}$ ,  $50\mu\text{m}$  and  $25\mu\text{m}$ ) were fabricated from these wafers using standard lithography and wet etching. Metal alloys were deposited both on the substrate side and on the top of the grown wafers to form n- and p- ohmic contacts, respectively. Optical windows were included to facilitate the injection of light into the devices in the photomultiplication measurements described below.

The values of the i-region widths of the  $\text{Al}_{0.48}\text{In}_{0.52}\text{As}$  wafers were estimated by fitting an electrostatic electric field model with piecewise continuous 3-region doping profiles to capacitance-voltage ( $C$ - $V$ ) characteristics measured on the fabricated devices. The  $C$ - $V$  characteristics of the InP devices indicate diffusion of the p-type dopant Zn from the  $\text{p}^+$  cladding into the i-regions. The values of  $w$  in equivalent ideal  $\text{p}^+\text{-i-n}^+$  diodes were therefore estimated using another technique, as described in the next section. Zn diffusion becomes more severe in MOCVD grown  $\text{n}^+\text{-i-p}^+$  wafers so that this growth technique is not suitable for InP wafers.

### Photomultiplication and Excess Noise measurements

Photomultiplication and excess noise measurements were performed on these devices using setups described in [1].

Optical injection into the InP diodes was achieved by focusing light from a 633nm He-Ne laser onto the top  $\text{p}^+$  cladding layer. It is estimated that more than 95% of this light is absorbed in this layer on the basis of the known optical absorption coefficients in doped InP [2]. This injection condition therefore enables measurement of pure electron multiplication and excess noise factors,  $M_e$  and  $F_e$ , respectively.

The measured pure electron multiplication factors of the five InP wafers versus reverse bias are shown in Figure 1, together with the results calculated using the local InP ionisation coefficients from [3] in the local impact ionisation model, in which dead space is neglected. The values of  $w$  were adjusted to fit the calculated results to the experimental data.

Photomultiplication experiments were performed using the same setup on the

$\text{Al}_{0.48}\text{In}_{0.52}\text{As}$  devices. Because of the absence of published optical absorption coefficients in  $\text{Al}_{0.48}\text{In}_{0.52}\text{As}$  it was necessary to check whether the intended pure electron injection was indeed achieved. Laser illumination with wavelengths of both 442nm and 542nm were used, with differing optical absorption coefficients, and the resulting multiplication factors were found to be indistinguishable, indicating that pure electron injection can be obtained using either wavelength. The measured pure electron multiplication factors as a function of reverse bias are shown in Figure 2.

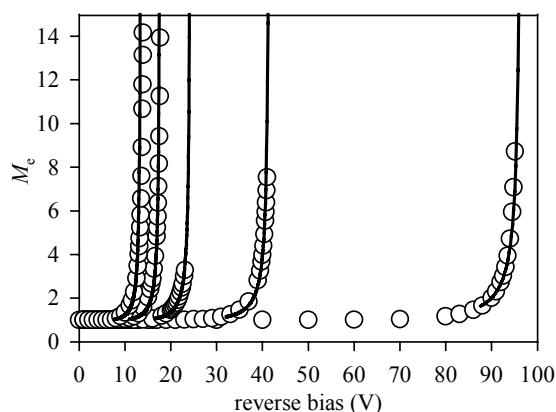


Figure 1: From right to left, (symbols)  $M_e(V)$  measured on the  $2.4\mu\text{m}$ ,  $0.9\mu\text{m}$ ,  $0.48\mu\text{m}$ ,  $0.33\mu\text{m}$  and  $0.24\mu\text{m}$  thick InP diodes. The lines are predictions using the local impact ionisation model with local InP ionisation coefficients.

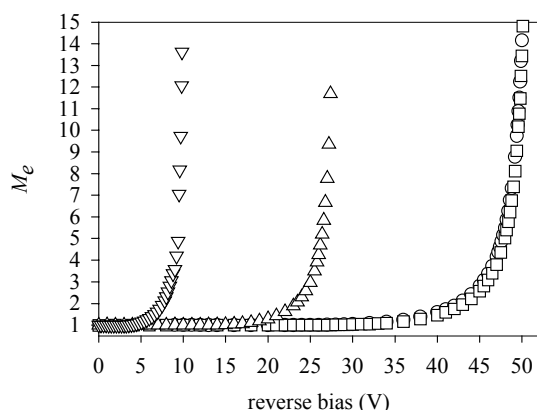


Figure 2:  $M_e(V)$  measured on the  $1.0\mu\text{m}$  AlInAs1 ( $\nabla$ ),  $1.0\mu\text{m}$  AlInAs4 ( $\boxtimes$ ),  $0.5\mu\text{m}$  ( $\rho$ ) and  $0.1\mu\text{m}$  ( $\sigma$ )  $\text{Al}_{0.48}\text{In}_{0.52}\text{As}$  diodes.

It can be observed from Figures 1 and 2 that

the breakdown voltages of the  $\text{Al}_{0.48}\text{In}_{0.52}\text{As}$  diodes are slightly higher than those of the InP diodes with similar i-region widths. The difference is illustrated in Figure 3, which shows breakdown voltages estimated from the measured multiplication curves versus i-region width. Using  $\text{Al}_{0.48}\text{In}_{0.52}\text{As}$  instead of InP as the avalanche region material in near IR APDs therefore requires slightly higher operating voltages.

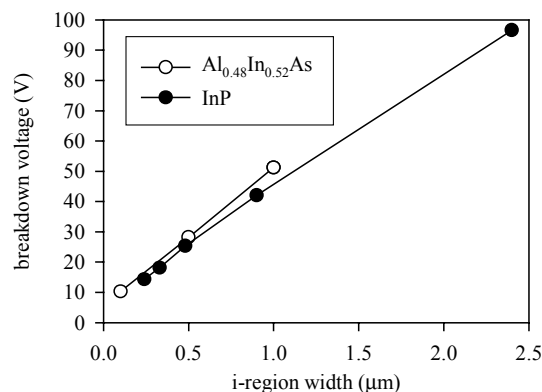


Figure 3: Breakdown voltages of  $\text{Al}_{0.48}\text{In}_{0.52}\text{As}$  and InP diodes estimated from the measured multiplication factor curves.

Since the excess noise introduced by the avalanche process determines the usefulness of an APD it is vital to compare the excess noise characteristics measured on the two materials and these are compared in Figure 4.

McIntyre calculated the excess noise factor as a function of multiplication in a local impact ionisation model and found this to depend only on the ratio of the ionisation coefficients and the carrier injection conditions [4]. To obtain lowest excess noise the electron and the hole ionisation coefficients,  $\alpha$  and  $\beta$ , respectively, should be widely dissimilar and the carrier type with higher ionisation coefficient should be injected [4].

The measurements of local ionisation coefficient on InP by Armiento *et al.* [3] established that  $\alpha < \beta$  so that the excess noise resulting from pure electron injection will be higher than from pure hole

injection. Since the noise measurements for the InP diodes used pure electron injection it is expected that excess noise measured from pure hole injection will be lower than the InP results shown in Figure 4. However the difference between the different injection conditions usually becomes small in devices with narrow i-region widths because they operate at high fields, where  $\alpha \approx \beta$ . On the other hand electron injection is preferred for the  $\text{Al}_{0.48}\text{In}_{0.52}\text{As}$  diodes because  $\alpha > \beta$  in this material [5].

Excess noise factors using the local model were predicted for the InP devices using the local InP ionisation coefficients [3] and McIntyre's equation [4], as shown in the solid lines in Figure 4. It can be seen that, while the predicted and measured  $F_e(M_e)$  of the  $w = 2.4\mu\text{m}$  InP device are in agreement, the local predictions significantly overestimate the excess noise factors for other devices, indicating the influence of dead space, which becomes more important in devices with narrow i-region widths and suppresses excess noise, regardless of carrier injection condition [6].

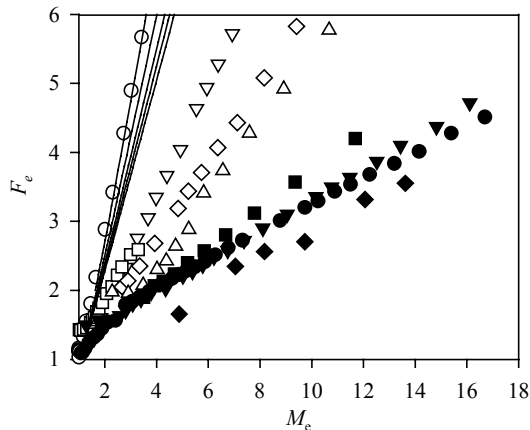


Figure 4: Comparison of the  $F_e(M_e)$  measured from the InP (open symbols,  $\circ$  for  $w = 2.4\mu\text{m}$ ,  $\square$  for  $w = 0.9\mu\text{m}$ ,  $\triangle$  for  $w = 0.48\mu\text{m}$ ,  $\diamond$  for  $w = 0.33\mu\text{m}$  and  $\nabla$  for  $w = 0.24\mu\text{m}$ ) and  $\text{Al}_{0.48}\text{In}_{0.52}\text{As}$  (closed symbols,  $\star$  for  $w = 1.0\mu\text{m}$  AllnAs1,  $\theta$  for  $w = 1.0\mu\text{m}$  AllnA4,  $\boxtimes$  for  $w = 0.5\mu\text{m}$  and  $\blacklozenge$  for  $w = 0.1\mu\text{m}$ ) wafers. Solid lines are the predicted local excess noise factors for the InP devices (from top to bottom,  $w = 2.4\mu\text{m}$ ,  $0.9\mu\text{m}$ ,  $0.48\mu\text{m}$ ,  $0.33\mu\text{m}$  and  $0.24\mu\text{m}$ ).

The behaviour of  $F_e(M_e)$  in the  $\text{Al}_{0.48}\text{In}_{0.52}\text{As}$  diodes as the i-region width reduces is less clear and may be caused by the competing effects of the changing  $\alpha$  and  $\beta$  and the increased importance of dead space. This results in  $F_e(M_e)$  roughly independent of i-region width in the  $\text{Al}_{0.48}\text{In}_{0.52}\text{As}$  devices, whereas the InP devices exhibit lower excess noise as the i-region width decreases for a given multiplication factor. In conclusion, it is clear that an InP APD should have a narrow avalanche region width to exploit the favourable effect of the dead space but  $\text{Al}_{0.48}\text{In}_{0.52}\text{As}$  APDs with different avalanche region widths can provide similar excess noise characteristics.

Comparison between the behaviour of  $F_e(M_e)$  in InP and in  $\text{Al}_{0.48}\text{In}_{0.52}\text{As}$  in Figure 4 suggests that, within the range of i-region widths studied here,  $\text{Al}_{0.48}\text{In}_{0.52}\text{As}$  APDs promise lower excess noise than InP.

### Summary and Future Directions

We have compared multiplication factors, breakdown voltages and excess noise factors measured on InP and  $\text{Al}_{0.48}\text{In}_{0.52}\text{As}$   $\text{p}^+\text{-i-n}^+$  diodes with varying avalanche region widths. For a given i-region width the InP  $\text{p}^+\text{-i-n}^+$  diodes have slightly lower breakdown voltages than the  $\text{Al}_{0.48}\text{In}_{0.52}\text{As}$  devices. The excess noise in the  $\text{Al}_{0.48}\text{In}_{0.52}\text{As}$   $\text{p}^+\text{-i-n}^+$  devices are lower than in the InP diodes with similar i-region widths, providing a means of reducing excess avalanche noise in near IR APDs.

The observations made in this work provide useful information for future design of III-V near IR APDs. Design of an  $\text{In}_{0.53}\text{Ga}_{0.47}\text{As}/\text{Al}_{0.48}\text{In}_{0.52}\text{As}$  APD is now underway.

The authors wish to acknowledge support of the Electromagnetic Remote Sensing

Defence Technology Centre, U. K. and the Engineering and Physical Sciences Research Council, U. K. for this work.

### References

- [1] J. S. Ng, "Avalanche Photodiodes," Year 1 annual report, for the project 'Avalanche Photodiodes' (EMRS/DTC/1/31), Chapter 3, Feb 2003.
- [2] D. E. Aspnes *et al.*, "Dielectric functions and optical parameters of Si, Ge, GaP, GaAs, GaSb, InP, InAs, and InSb from 1.5 to 6.0eV," *Phys. Rev. B (USA)*, **27**(2), p. 251-253, 1983.
- [3] C. A. Armiento and S. H. Groves, "Impact ionisation in (100)-, (110)-, and (111)-oriented InP avalanche photodiodes," *Appl. Phys. Lett.*, **43**(2), p. 198-200, 1983.
- [4] R. J. McIntyre, "Multiplication noise in uniform avalanche diodes," *IEEE Trans. Electron Devices*, **ED-13**(1), p. 164-168, 1966.
- [5] I. Watanabe, T. Torikai, K. Makita, K. Fukushima and T. Uji, "Impact ionization rates in (100)  $\text{Al}_{0.48}\text{In}_{0.52}\text{As}$ ," *IEEE Electron Device Lett.*, **11**(10), pp. 437-438, Oct. 1990.
- [6] K. F. Li *et al.*, "Avalanche multiplication noise characteristics in thin GaAs  $\text{p}^+\text{-i-n}^+$  diodes," *IEEE Trans. Electron Devices*, **45**(10), p. 2102-2107, 1998.